Coordination of Carbon Monoxide and Isocyanides to Bis(pentamethylcyclopentadienyl)ytterbium and Related Bivalent Ytterbocenes

Madeleine Schultz, Carol J. Burns, David J. Schwartz, and Richard A. Andersen*,[1]

Chemistry Department and Chemical Sciences Division of Lawrence Berkeley National Laboratory, University of California, Berkeley, California 94720

Received July 24, 2001

Changes in the infrared spectra of methylcyclohexane solutions of the base-free ytterbocenes $(Me_5C_5)_2Yb$, $[1,3\text{-}(Me_3C)_2C_5H_3]_2Yb$, and $[1,3\text{-}(Me_3Si)_2C_5H_3]_2Yb$ in the presence of CO show that carbonyl adducts are formed at room temperature. The adducts are formed reversibly, and they have not been isolated. The ν_{CO} values are lower than that of free CO for the adducts of $(Me_5C_5)_2Yb$ and $[1,3\text{-}(Me_3C)_2C_5H_3]_2Yb$, and in the case of $(Me_5C_5)_2Yb$ the ^{13}C NMR resonance of the carbonyl is deshielded from that of free CO, indicating that CO is acting as a net π-acceptor ligand in those molecules. The ν_{CO} value for the adduct of $[1,3\text{-}(Me_3Si)_2C_5H_3]_2Yb$ is slightly higher than that of free CO, which demonstrates that changing the substituents on the cyclopentadienyl rings can alter the electron richness of the ytterbocene. Isocyanide complexes of these ytterbocenes and of $(Me_4C_5H)_2Yb$ have been isolated and fully characterized, including by X-ray crystallography for $(Me_5C_5)_2Yb(2,6\text{-}Me_2C_6H_3NC)_2$, $[1,3\text{-}(Me_3C)_2C_5H_3]_2Yb(2,6\text{-}Me_2C_6H_3NC)_2$, and $[1,3\text{-}(Me_3Si)_2C_5H_3]_2Yb(2,6\text{-}Me_2C_6H_3NC)_2$. The solution electronic spectra (350−1000 nm) for the base-free ytterbocenes and their carbonyl and isocyanide adducts have been measured and interpreted according to a molecular orbital model. All of the data are consistent with the notion that ytterbium(II) metallocenes can act as net π-donor fragments.

Downloaded by CARLI CONSORTIUM on June 29, 2009
Published on November 27, 2001 on http://pubs.acs.org | doi: 10.1021/om0106579

Introduction

There are no reported examples of isolable lanthanide carbonyl complexes.[2] In an argon matrix, lanthanide and actinide carbonyls have been observed in which ν_{CO} is reduced from that of free CO.[3−7] Evans has reported that $(Me_5C_5)_2Sm$ and CO react in THF to form a bimetallic Sm(III) species with the metal atoms bridged by an O_2C_3O ligand which is presumed to arise from the CO.[8] Two molecular carbonyl adducts of tris(cyclopentadienyl)uranium (Cp'_3U) compounds are known; in both cases adduct formation is reversible, and only one has been isolated as a crystalline solid, $(Me_4C_5H)_3UCO$.[9−11] The values of ν_{CO} in these adducts, 1976 and 1900 cm^{-1} for $(Me_3SiC_5H_4)_3UCO$ and $(Me_4C_5H)_3UCO$, respectively, are much lower than in free CO (2136 cm^{-1} in methylcyclohexane solution), consistent with the view that tris(cyclopentadienyl)uranium fragments can be excellent π-donors. The lanthanide elements do not interact with ligands such as CO as well as their actinide congeners, since the valence 4f orbitals are more spatially compact and better shielded by the core electrons relative to the 5f orbitals of actinide metals. This is illustrated by the greatly reduced stretching frequency of the carbonyl adducts just described, compared with the lack of adduct formation with CO of the Cp'_3Ce and Cp'_3Nd molecules having identical cyclopentadienyl ligands.[11] This difference may be rationalized by comparing the relative polarizabilities of the 4f and 5f electrons; the greater radial extent of the 5f orbitals makes the electrons in those orbitals more polarizable. The bivalent lanthanides are more polarizable than the trivalent lanthanides, however, and their ionization energies are lower than those of the trivalent lanthanides, due to the lower effective nuclear charge. These concepts can be illustrated by examination of the gas-phase photoelectron spectroscopy of the cyclopentadienyl derivatives of these metals, which gives experimental values for the relative f orbital ionization energies. The ionization of electrons in f orbitals is not observed in $(MeC_5H_4)_3M$ (M being a

(1) To whom correspondence should be addressed at the Chemistry Department, University of California, Berkeley, CA 94720. E-mail: raandersen@lbl.gov.

(2) Ellis, J. E.; Beck, W. *Angew. Chem., Int. Ed. Engl.* **1995**, *34*, 2489−2491.

(3) Sheline, R. K.; Slater, J. L. *Angew. Chem., Int. Ed. Engl.* **1975**, *14*, 309−313.

(4) Slater, J. L.; DeVore, T. C.; Calder, V. *Inorg. Chem.* **1973**, *12*, 1918−1921.

(5) Slater, J. L.; DeVore, T. C.; Calder, V. *Inorg. Chem.* **1974**, *13*, 1808−1812.

(6) Zhou, M.; Andrews, L.; Li, J.; Bursten, B. E. *J. Am. Chem. Soc.* **1999**, *121*, 9712−9721.

(7) Zhou, M.; Andrews, L.; Li, J.; Bursten, B. E. *J. Am. Chem. Soc.* **1999**, *121*, 12188−12189.

(8) Evans, W. J.; Grate, J. W.; Hughes, L. A.; Zhang, H.; Atwood, J. L. *J. Am. Chem. Soc.* **1985**, *107*, 3728−3730.

(9) Brennan, J. G.; Andersen, R. A.; Robbins, J. L. *J. Am. Chem. Soc.* **1986**, *108*, 335−336.

(10) Parry, J.; Carmona, E.; Coles, S.; Hursthouse, M. *J. Am. Chem. Soc.* **1995**, *117*, 2649−2650.

(11) del Mar Conejo, M.; Parry, J. S.; Carmona, E.; Schultz, M.; Brennan, J. G.; Beshouri, S. M.; Andersen, R. A.; Rogers, R. D.; Coles, S.; Hursthouse, M. *Chem. Eur. J.* **1999**, *5*, 3000−3009.

10.1021/om0106579 CCC: $20.00 © 2001 American Chemical Society
Publication on Web 11/27/2001

Downloaded by CARLI CONSORTIUM on June 29, 2009
Published on November 27, 2001 on http://pubs.acs.org | doi: 10.1021/om0106579

lanthanide metal) prior to the onset of the ring Cp(π) ionizations at about 7 eV. In comparison, the f ionization in $Cp'_3U(THF)$ occurs at about 6.4 eV, indicating that the 5f electrons are easier to ionize, and presumably also to polarize, than the 4f electrons of trivalent metallocenes.[12] The f orbital ionizations in the bivalent lanthanide metallocenes $(Me_5C_5)_2M$ are observed in the range 6−6.5 eV, and the ionization energy of the ytterbium complex is lower than that of the europium complex by 0.2 eV.[13] Thus, ytterbium(II) in a metallocene such as $(Me_5C_5)_2Yb$ is the most likely lanthanide metal to engage in back-donation with appropriate π-acceptors such as acetylenes, olefins, and CO.

The structure of $(Me_5C_5)_2Yb$ is bent in both the solid state and the gas phase.[14,15] Little reorganization is required to coordinate another ligand; therefore, the enthalpy of coordination does not have to compensate a large reorganization enthalpy. Therefore, both geometric and electronic factors suggest that $(Me_5C_5)_2Yb$ is likely to bind to weakly Lewis basic ligands. The two other soluble base-free substituted ytterbocenes, $[1,3\text{-}(Me_3C)_2C_5H_3]_2Yb$[15] and $[1,3\text{-}(Me_3Si)_2C_5H_3]_2Yb$,[16] are also bent in the solid state and may be expected to form similar adducts.

Bis(pentamethylcyclopentadienyl)ytterbium forms isolable 1:1 complexes with disubstituted acetylenes, which are the only reported examples of lanthanide−acetylene complexes.[17] The electron-rich ethylene $(PPh_3)_2Pt(C_2H_4)$ coordinates to $(Me_5C_5)_2Yb$, giving a molecule in which ethylene bridges the two metal centers.[18] The platinum−ethylene complex was used, since ethylene itself (10 atm) reacts with $(Me_5C_5)_2Yb$ in hexane solution at room temperature to form polyethylene.[19] This is similar to the behavior of $(Me_5C_5)_2Sm$, which also polymerizes ethylene.[20] In the course of the ethylene binding and polymerization studies, it was shown that carbon monoxide inhibits ethylene polymerization. Thus, addition of ethylene (to total pressure of 10 atm) to a solution of $(Me_5C_5)_2Yb$ in hexane under CO pressure (5 atm) does not produce polyethylene. Instead, the solution remains homogeneous and perceptibly green. Removal of the gases followed by addition of ethylene yields polyethylene instantaneously.[19] This observation suggests that CO is a better ligand for $(Me_5C_5)_2Yb$ than ethylene, but the extent of the interaction is difficult to quantify.

In this paper, we report the formation of carbonyl adducts of the ytterbocene complexes $(Me_5C_5)_2Yb$, $[1,3\text{-}(Me_3C)_2C_5H_3]_2Yb$, and $[1,3\text{-}(Me_3Si)_2C_5H_3]_2Yb$ in methylcyclohexane solution. No structural information is available, since the carbonyl adducts are labile. To model this reaction, the reactions of the ytterbocenes with several isocyanides were studied, since isocyanides and CO are structurally and electronically related.

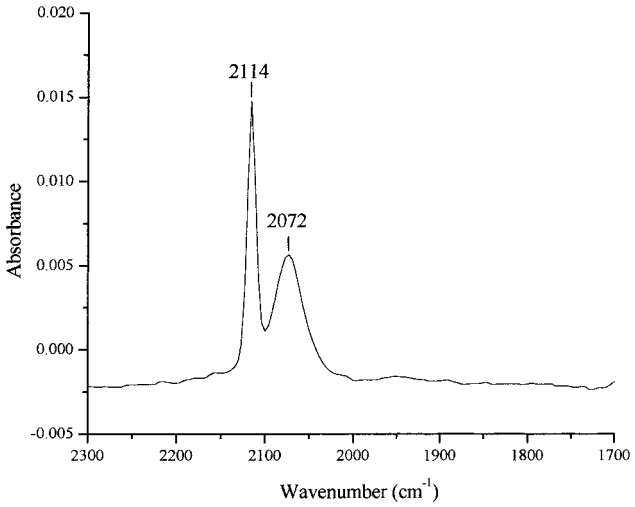

Figure 1. Infrared spectrum of $(Me_5C_5)_2Yb$ in methylcyclohexane under 1 atm of CO. This spectrum is background-corrected for solvent and CO.

Results

Carbonyl Complexes. A dark brown methylcyclohexane solution of base-free $(Me_5C_5)_2Yb$ turns deep brown-green on exposure to 1 atm of carbon monoxide with stirring at 25 °C. The infrared spectrum of the solution under a CO atmosphere (see Experimental Section for details) contains two absorption peaks at 2114 cm^{-1} ($\nu_{1/2}$ = 10 cm^{-1}) and 2072 cm^{-1} ($\nu_{1/2}$ = 35 cm^{-1}) (Figure 1). Exposure of the solution to vacuum followed by dinitrogen results in the disappearance of the peaks; they reappear when the solution is again exposed to carbon monoxide. This cycle can be repeated at least four times before decomposition of the air-sensitive starting material occurs. The $(Me_5C_5)_2Yb$ starting material can be recrystallized unchanged after an exposure to CO, showing that the reaction is reversible. The two peaks in the infrared spectrum appear to correspond to two discrete carbonyl complexes that are in equilibrium with each other. Extensive pressure- and temperature-dependence studies have been carried out as part of a quantitative study of the equilibrium.[21] The results of those studies indicate that the peak at 2114 cm^{-1} corresponds to a 1:1 complex that forms at lower pressures, which is in equilibrium with a 1:2 complex giving rise to the peak at 2072 cm^{-1}. Both of these carbonyl complexes have CO stretching frequencies lower than that of free carbon monoxide in methylcyclohexane (2136 cm^{-1}) (Table 1). The observation that ν_{CO} for the apparent dicarbonyl species is lower and broader than that for the monocarbonyl has precedent in matrix-isolated atom (Th, U) carbonyl species where $\nu_{CO}[M(CO)_2] < \nu_{CO}[M(CO)_1]$.[6,7] A similar observation was made for zirconium and hafnium carbonyls in a cryogenic matrix.[22]

It is of interest to compare this result with the corresponding experiment on $(Me_5C_5)_2Ca$.[23] In this case,

(12) Green, J. C. *Struct. Bonding* **1981**, *43*, 37−112.
(13) Green, J. C.; Hohl, D.; Rösch, N. *Organometallics* **1987**, *6*, 712−720.
(14) Andersen, R. A.; Blom, R.; Boncella, J. M.; Burns, C. J.; Volden, H. V. *Acta Chem. Scand., Ser. A* **1987**, *A41*, 24−35.
(15) Schultz, M.; Burns, C. J.; Schwartz, D. J.; Andersen, R. A. *Organometallics* **2000**, *19*, 781−789.
(16) Hitchcock, P. B.; Howard, J. A. K.; Lappert, M. F.; Prashar, S. *J. Organomet. Chem.* **1992**, *437*, 177−189.
(17) Burns, C. J.; Andersen, R. A. *J. Am. Chem. Soc.* **1987**, *109*, 941−942.
(18) Burns, C. J.; Andersen, R. A. *J. Am. Chem. Soc.* **1987**, *109*, 915−917.
(19) Burns, C. J. Ph.D. Thesis, University of California, Berkeley, CA, 1987.
(20) Evans, W. J.; Decoster, D. M.; Greaves, J. *Macromolecules* **1995**, *28*, 7929−7936.
(21) Selg, P.; Brintzinger, H. H.; Andersen, R. A. Manuscript in preparation.
(22) Zhou, M.; Andrews, L. *J. Am. Chem. Soc.* **2000**, *122*, 1531−1539.

Table 1. Infrared Data for Carbonyl and Isocyanide Complexes of Base-Free Ytterbocenes

complex	ν_{CO} or ν_{CN} (cm^{-1})	ν_{CO}(complex) − ν_{CO}(free CO) or ν_{CN}(complex) − ν_{CN}(free CNR)
$(Me_5C_5)_2Yb(CO)_n$	2114, 2072	−22, −64
$[1,3\text{-}(Me_3C)_2C_5H_3]_2Yb(CO)$	2126	−10
$[1,3\text{-}(Me_3Si)_2C_5H_3]_2Yb(CO)$	2138	+2
$(Me_5C_5)_2Yb(2,6\text{-}Me_2C_6H_3NC)_2$	2131	+13
$(Me_5C_5)_2Yb(Me_3CNC)_2$	2160	+26
$(Me_5C_5)_2Yb(C_6H_{11}NC)_2$	2164	+26
$[1,3\text{-}(Me_3C)_2C_5H_3]_2Yb(2,6\text{-}Me_2C_6H_3NC)_2$	2129	+11
$[1,3\text{-}(Me_3C)_2C_5H_3]_2Yb(Me_3CNC)_2$	2161	+27
$[1,3\text{-}(Me_3C)_2C_5H_3]_2Yb(C_6H_{11}NC)_2$	2166	+28
$[1,3\text{-}(Me_3Si)_2C_5H_3]_2Yb(2,6\text{-}Me_2C_6H_3NC)_2$	2142	+24
$[1,3\text{-}(Me_3Si)_2C_5H_3]_2Yb(C_6H_{11}NC)_2$	2168	+30
$(Me_4C_5H)_2Yb(2,6\text{-}Me_2C_6H_3NC)_2$	2132	+14
$(Me_4C_5H)_2Yb(Me_3CNC)_2$	2162	+28
$(Me_4C_5H)_2Yb(C_6H_{11}NC)_2$	2173	+35

Table 2. Solution Optical Data for Base-Free Ytterbocenes and Their Carbonyl and Isocyanide Complexes

complex	λ_{max}, nm (ϵ, L mol^{-1} cm^{-1})
$(Me_5C_5)_2Yb$[a]	751 (173), 515 (277), 474 (374), 429 (610)
$(Me_5C_5)_2Yb + CO$[a]	699 (256), 520 (436), 472 (540), 425 (831)
$(Me_5C_5)_2Yb$	736 (221), 547 (277), 429 (665)
$(Me_5C_5)_2Yb + CO$	733 (249), 425 (754)
$[1,3\text{-}(Me_3C)_2C_5H_3]_2Yb$[a]	655 (228), 453 (537), 396 (540)
$[1,3\text{-}(Me_3C)_2C_5H_3]_2Yb + CO$[a]	653 (171), 451 (440), 396 (483)
$[1,3\text{-}(Me_3Si)_2C_5H_3]_2Yb$[a]	648 (244), 468 (404), 392 (584)
$[1,3\text{-}(Me_3Si)_2C_5H_3]_2Yb + CO$[a]	645 (168), 463 (320), 391 (500)
$(Me_5C_5)_2Yb(2,6\text{-}Me_2C_6H_3NC)_2$	776 (610), 434 (1114)
$(Me_5C_5)_2Yb(Me_3CNC)_2$	955 (137), 450 (676)
$(Me_5C_5)_2Yb(C_6H_{11}NC)_2$	942 (234), 453 (963)
$[1,3\text{-}(Me_3C)_2C_5H_3]_2Yb(2,6\text{-}Me_2C_6H_3NC)_2$	586 (755), 390 (1086)
$[1,3\text{-}(Me_3C)_2C_5H_3]_2Yb(Me_3CNC)_2$	648 (197), 397 (692)
$[1,3\text{-}(Me_3C)_2C_5H_3]_2Yb(C_6H_{11}NC)_2$	606 (260), 399 (916)
$[1,3\text{-}(Me_3Si)_2C_5H_3]_2Yb(2,6\text{-}Me_2C_6H_3NC)_2$	617 (533), 389 (1111)
$[1,3\text{-}(Me_3Si)_2C_5H_3]_2Yb(C_6H_{11}NC)_2$	830 (234), 431 (1059)
$(Me_4C_5H)_2Yb(2,6\text{-}Me_2C_6H_3NC)_2$	776 (952), 448 (1251)
$(Me_4C_5H)_2Yb(C_6H_{11}NC)_2$	950 (252), 458 (968)

[a] In methylcyclohexane solution; for all other cases, toluene is the solvent.

Downloaded by CARLI CONSORTIUM on June 29, 2009
Published on November 27, 2001 on http://pubs.acs.org | doi: 10.1021/om0106579

exposure of a solution of $(Me_5C_5)_2Ca$ in toluene to CO pressures of 2.5−70 bar gives rise to a single ν_{CO} band at 2158 cm^{-1}, which is 22 cm^{-1} higher than the value for free CO. This process is reversible, and the adduct has a 1:1 stoichiometry. The radii of Ca(II) and Yb(II) are similar,[24] and the structures of their decamethylmetallocenes in the solid state and the gas phase are also similar.[14,15,25] However, changing from the $3d^0$ metal calcium to the $4f^{14}$ $5d^0$ metal ytterbium alters the behavior of these two decamethylmetallocenes toward carbon monoxide.

Since the color of a solution of $(Me_5C_5)_2Yb$ in methylcyclohexane changes upon exposure to CO, the optical spectrum of the $(Me_5C_5)_2Yb$ solution was measured in a separate experiment. Base-free $(Me_5C_5)_2Yb$ has four absorbances at 751, 515, 474, and 429 nm, all of which have similar extinction coefficients (Table 2). The highest wavelength absorption is thought to correspond to the HOMO−LUMO transition, and the three lower wavelength features are due to higher energy ligand field transitions.[13] Upon brief exposure of the cuvette to vacuum followed by back-filling with carbon monoxide, the HOMO−LUMO transition is blue-shifted to 699 nm (Figure 2). This procedure is also reversible, although the peaks become broad and some resolution is lost, probably due to decomposition of the sample, since the solute concentration is small. In toluene solution, the HOMO−LUMO transition of $(Me_5C_5)_2Yb$ is observed at 736 nm, and the spectrum does not change significantly when carbon monoxide is added (Figure 2). This indicates that toluene may be competing with, or inhibiting, carbon monoxide binding.

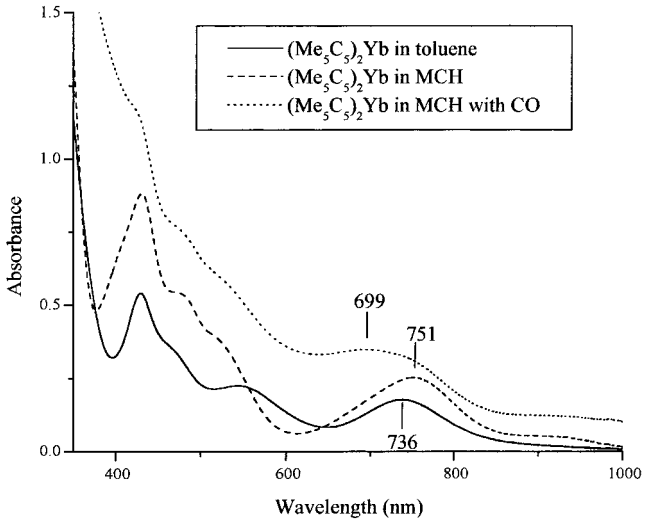

Figure 2. UV−visible spectra of $(Me_5C_5)_2Yb$ in toluene and methylcyclohexane under N_2 and in methylcyclohexane under 1 atm of CO.

(23) Selg, P.; Brintzinger, H. H.; Andersen, R. A.; Horvath, I. T. *Angew. Chem., Int. Ed. Engl.* **1995**, *34*, 791−793.
(24) Shannon, R. D. *Acta Crystallogr., Sect. A* **1976**, *A32*, 751−767.
(25) Williams, R. A.; Hanusa, T. P.; Huffman, J. C. *Organometallics* **1990**, *9*, 1128−1134.

Downloaded by CARLI CONSORTIUM on June 29, 2009
Published on November 27, 2001 on http://pubs.acs.org | doi: 10.1021/om0106579

The $^{13}C\{^1H\}$ NMR chemical shift of a saturated solution of ^{13}CO in methylcyclohexane-d_{14} is 185.0 ppm ($\nu_{1/2}$ = 4 Hz). When a methylcyclohexane-d_{14} solution of $(Me_5C_5)_2Yb$ is exposed to 1 atm of ^{13}CO, the new chemical shift is δ 203 ppm ($\nu_{1/2}$ = 425 Hz), a significant downfield shift. The broadness of the resonance indicates that some exchange process is occurring with a rate that is on the order of the NMR time scale at 25 °C. Cooling the sample leads to a downfield shift and broadening of the CO resonance; at −30 °C, δ_{CO} 215 ppm and $\nu_{1/2}$ = 2200 Hz. In the temperature range −70 to −88 °C, the CO resonance decoalesces into two resonances; at −73 °C, δ_{CO} 225 ppm and $\nu_{1/2}$ = 650 Hz, and at −88 °C, δ_{CO} 239 and 198 ppm, both with $\nu_{1/2}$ = 580 Hz. As the sample is cooled further, the lower field CO resonance broadens considerably, while the higher field CO resonance sharpens. In addition, the Me_5C_5 methyl resonance decoalesces into two resonances; the ring carbon resonance may also decoalesce, but the resolution of the spectrum is insufficient to state this unequivocally. Finally, at −107 °C the $^{13}C\{^1H\}$ spectrum contains two sets of resonances for the CO and Me_5C_5 methyl groups: δ 243 ppm ($\nu_{1/2}$ = 2800 Hz), δ 199 ppm ($\nu_{1/2}$ = 100 Hz); δ 11.2 ppm ($\nu_{1/2}$ = 90 Hz), δ 9.0 ppm ($\nu_{1/2}$ = 50 Hz), while a Me_5C_5 ring resonance appears at δ 113 ppm ($\nu_{1/2}$ = 50 Hz). These changes in the spectra are fully reversible and do not occur when a sample of $(Me_5C_5)_2Yb$ under a nitrogen atmosphere is cooled. The NMR data are consistent with the formation of two discrete adducts of $(Me_5C_5)_2Yb$ with CO, as was deduced from infrared spectroscopy.

The $^{13}C\{^1H\}$ NMR spectrum of a saturated methylcyclohexane-d_{14} solution of $(Me_5C_5)_2Yb$ under natural isotopic abundance CO varies with pressure. The changes in chemical shifts of both the ring and methyl carbon atoms are nonlinear with pressure, although saturation is not reached up to 220 psi. The chemical shift changes are reversible; exposure of the NMR tube to vacuum followed by dinitrogen results in return of the chemical shifts to their original values.

To probe the effect of ring substitution on the metal−ligand interaction, the infrared spectroscopic experiments have been repeated with other ytterbocene complexes. A green-brown methylcyclohexane solution of $[1,3\text{-}(Me_3C)_2C_5H_3]_2Yb$, when exposed to 1 atm of carbon monoxide, produces a single peak at 2128 cm^{-1} ($\nu_{1/2}$ = 10 cm^{-1}) in the infrared spectrum. The peak disappears upon exposure of the solution to vacuum followed by dinitrogen. Similarly, when a solution of $[1,3\text{-}(Me_3Si)_2C_5H_3]_2Yb$ in methylcyclohexane is stirred under carbon monoxide, a peak is observed in the infrared spectrum at 2138 cm^{-1} ($\nu_{1/2}$ = 8 cm^{-1}). Again, the reaction is reversible and only a single absorption band is observed for the carbonyl adducts of both of these ytterbocenes.

The infrared data for the CO adducts of the three ytterbocenes are collected in Table 1. It can be seen that the CO stretch is reduced from that of free CO in the cases of $(Me_5C_5)_2Yb$ and $[1,3\text{-}(Me_3C)_2C_5H_3]_2Yb$, while in the case of $[1,3\text{-}(Me_3Si)_2C_5H_3]_2Yb$, the CO adduct has a stretching frequency only 2 cm^{-1} higher than the free ligand. The only difference between these molecules is the substitution of the cyclopentadienide rings; the better donor substituents on the rings lower ν_{CO}.[26]

The optical spectra of the other base-free metallocenes have been examined. The optical spectrum of $[1,3\text{-}(Me_3C)_2C_5H_3]_2Yb$ in methylcyclohexane has a HOMO−LUMO transition at 655 nm, while that of $[1,3\text{-}(Me_3Si)_2C_5H_3]_2Yb$ is observed at 648 nm. Exposure of the cuvette to carbon monoxide does not alter the spectra of either of these ytterbocenes (Table 2). The molecule $[1,3\text{-}(Me_3Si)_2C_5H_3]_2Yb$ is purple in the solid state, although in solution it is olive brown. Optical data for the three metallocenes as well as their CO adducts are shown in Table 2.

Isocyanide Complexes. Isocyanide complexes of $(Me_5C_5)_2Yb$, $[1,3\text{-}(Me_3C)_2C_5H_3]_2Yb$, and $[1,3\text{-}(Me_3Si)_2C_5H_3]_2Yb$ as well as $(Me_4C_5H)_2Yb$ are prepared from the corresponding etherates, $Cp'_2Yb(OEt_2)$, in toluene (eq 1). The 1:2 adducts are relatively insoluble in aromatic

$$Cp'_2Yb(OEt_2) + 2CNR \xrightarrow{\text{toluene}} Cp'_2Yb(CNR)_2 \quad (1)$$

$Cp' = Me_5C_5$, $1,3\text{-}(Me_3C)_2C_5H_3$, $1,3\text{-}(Me_3Si)_2C_5H_3$, Me_4C_5H

$R = 2,6\text{-}Me_2C_6H_3$, Me_3C, C_6H_{11}

and aliphatic solvents and can be crystallized from toluene as dark red ($Cp' = Me_5C_5$, $1,3\text{-}(Me_3C)_2C_5H_3$, $1,3\text{-}(Me_3Si)_2C_5H_3$, Me_4C_5H; $R = C_6H_{11}$, Me_3C), blue ($Cp' = 1,3\text{-}(Me_3C)_2C_5H_3$, $1,3\text{-}(Me_3Si)_2C_5H_3$; $R = 2,6\text{-}Me_2C_6H_3$), or green ($Cp' = Me_5C_5$, Me_4C_5H; $R = 2,6\text{-}Me_2C_6H_3$) blocks.

Infrared data for the isocyanide complexes are presented in Table 1. The infrared spectra contain a single, sharp CN stretch ($\nu_{1/2}$ between 12 and 20 cm^{-1}) in both the solid state and toluene solution for each adduct. This contrasts with the expected result for a metal center bound to two isocyanide ligands, as both a symmetric stretch and an asymmetric stretch are infrared active in idealized C_{2v} symmetry. One explanation for this observation is that the two isocyanide ligands are not electronically or mechanically coupled. The observed values of ν_{CN} for the isocyanide adducts are higher in frequency than those of the free isocyanides, but the changes are much less than for the previously reported isocyanide complexes $(C_5H_5)_3LnC_6H_{11}NC$ (Ln = La−Lu) of trivalent lanthanide metals, for which ν_{CN} increases between 60 and 74 cm^{-1} on coordination.[27,28] For a given ytterbocene fragment, the complex with $2,6\text{-}Me_2C_6H_3$-NC as the isocyanide ligand has its CN stretching frequency increased from that of the free ligand to a lesser extent than the complexes derived from aliphatic isocyanide ligands. This is most reasonably associated with the electron-withdrawing nature of the aryl group, making $2,6\text{-}Me_2C_6H_3NC$ a weaker electron donor. Isocyanide complexes with a 1:1 stoichiometry cannot be isolated; mixing an ytterbocene with 1 equiv of an isocyanide ligand results in the isolation of the 1:2 isocyanide complex and the ytterbocene starting complex.

It is interesting to compare $(Me_5C_5)_2Yb(2,6\text{-}Me_2C_6H_3\text{-}NC)_2$ with the analogous calcium complex, $(Me_5C_5)_2Ca$-

(26) Hays, M. L.; Hanusa, T. P. *Adv. Organomet. Chem.* **1997**, *40*, 117−170.
(27) Fischer, E. O.; Fischer, H. *J. Organomet. Chem.* **1966**, *6*, 141−148.
(28) von Ammon, R.; Kanellakopulos, B. *Ber. Bunsen-Ges. Phys. Chem.* **1972**, *76*, 995−999.

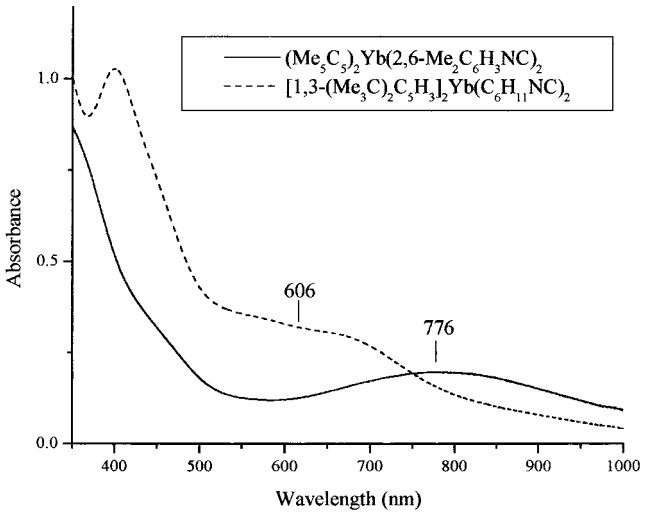

Figure 3. UV−visible spectra of $(Me_5C_5)_2Yb_2Yb(2,6\text{-}Me_2C_6H_3NC)_2$ and $[1,3\text{-}(Me_3C)_2C_5H_3](C_6H_{11}NC)_2$ in toluene.

$(2,6\text{-}Me_2C_6H_3NC)_2$.[29] In the calcium adduct, the CN stretching frequency of the complex is increased by 30 cm^{-1} relative to the free ligand, while the CN stretching frequency increases by only 13 cm^{-1} in the ytterbium adduct. A similar trend was found in the behavior of these metallocenes with CO as described above.

The optical spectra of the isocyanide complexes have been measured to investigate the dramatically different colors observed. Data are presented in Table 2. The position of the band assigned as the HOMO−LUMO transition depends on the substituents on the cyclopentadienide rings and on the isocyanide ligand. The bands for the isocyanide complexes are all very broad with $\nu_{1/2}$ = 200 nm or more (Figure 3).

The ^1H NMR spectrum of the adduct $(Me_5C_5)_2Yb(2,6\text{-}Me_2C_6H_3NC)_2$ has broad peaks at room temperature (Me_5C_5, $\nu_{1/2}$ = 5 Hz; Me_2C_6, $\nu_{1/2}$ = 3 Hz). Solid-state magnetic susceptibility measurements on this molecule show that it is diamagnetic, indicating that the broadened signals are probably due to chemical exchange. Variable-temperature ^1H NMR experiments have been carried out on this adduct both with and without added isocyanide ligand. Adding an excess of isocyanide causes the room-temperature resonances to broaden further; warming this sample to +70 °C causes the resonances to sharpen, indicating that the rate of exchange is increasing. When the sample is cooled, the resonances remain unchanged to −50 °C; below that temperature the signals begin to sharpen as the exchange between free and bound ligand is slowed. The stopped exchange region cannot be reached. The ^1H NMR spectra of all the other isocyanide complexes of the ytterbocenes also have broad peaks at room temperature, indicating that intermolecular exchange is occurring; in no case can the exchange be stopped by lowering the temperature.

The structures of three of the $2,6\text{-}Me_2C_6H_3NC$ complexes have been determined by X-ray crystallography. Important structural data are presented in Table 3, and the data collection parameters are shown in Table 4. Each molecule crystallizes as a monomer, and the overall structures are unsurprising, yet there are important differences in how the isocyanide ligands are arranged relative to the two cyclopentadienide rings. ORTEP diagrams of the three molecules are shown in Figures 4−6.

For the two molecules with disubstituted cyclopentadienide rings, the centroid−metal−centroid angles are similar, yet the twist angle of the two cyclopentadienide rings changes from eclipsed in the Me_3C example to

(29) Burns, C. J.; Andersen, R. A. *J. Organomet. Chem.* **1987**, *325*, 31−37.

Table 3. Selected Bond Lengths (Å) and Angles (deg) for $(Me_5C_5)_2Yb(2,6\text{-}Me_2C_6H_3NC)_2$, $[1,3\text{-}(Me_3C)_2C_5H_3]_2Yb(2,6\text{-}Me_2C_6H_3NC)_2$, and $[1,3\text{-}(Me_3Si)_2C_5H_3]_2Yb(2,6\text{-}Me_2C_6H_3NC)_2$

	$(Me_5C_5)_2Yb(2,6\text{-}Me_2C_6H_3NC)_2$	$[1,3\text{-}(Me_3C)_2C_5H_3]_2Yb(2,6\text{-}Me_2C_6H_3NC)_2$	$[1,3\text{-}(Me_3Si)_2C_5H_3]_2Yb(2,6\text{-}Me_2C_6H_3NC)_2$
Yb−C(ring) (mean)	2.69	2.72	2.70
Yb−Cp(centroid)	2.41	2.44	2.42
Cp−Yb−Cp	145	133	137
twist angle	8.7	1.0	34.0
$Yb-C_{CNR}$ (mean)	2.538(4)	2.61	2.56
$C_{CNR}-N$ (mean)	1.165(5)	1.15	1.16
$N-C_R$ (mean)	1.403(4)	1.40	1.42
$C_{CNR}-Yb-C_{CNR}$	91.7(2)	79.9(1)	90.5(2)
$Yb-C_{CN}-N$ (mean)	167.3(3)	171.7	176.4

Table 4. Selected Crystal Data and Data Collection Parameters for $(Me_5C_5)_2Yb(2,6\text{-}Me_2C_6H_3NC)_2$, $[1,3\text{-}(Me_3C)_2C_5H_3]_2Yb(2,6\text{-}Me_2C_6H_3NC)_2$, and $[1,3\text{-}(Me_3Si)_2C_5H_3]_2Yb(2,6\text{-}Me_2C_6H_3NC)_2$

	$(Me_5C_5)_2Yb(2,6\text{-}Me_2C_6H_3NC)_2$	$[1,3\text{-}(Me_3C)_2C_5H_3]_2Yb(2,6\text{-}Me_2C_6H_3NC)_2$	$[1,3\text{-}(Me_3Si)_2C_5H_3]_2Yb(2,6\text{-}Me_2C_6H_3NC)_2$
formula	$YbC_{38}H_{48}N_2$	$YbC_{44}H_{60}N_2$	$YbC_{40}Si_4H_{60}N_2$
fw	705.85	790.01	854.31
color	green	blue	blue
space group	*Pbcn* (No. 60)	$P\bar{1}$ (No. 2)	*Pbca* (No. 61)
a (Å)	14.7091(1)	11.4729(6)	19.9719(9)
b (Å)	15.5227(2)	11.6642(6)	20.6253(9)
c (Å)	14.6848(1)	16.0596(8)	22.099(1)
α (deg)	90	76.607(1)	90
β (deg)	90	86.592(1)	90
γ (deg)	90	72.470(1)	90
V (Å^3)	3352.91(4)	1993.5(2)	9103(1)
Z	4	2	8
temp (K)	168	113	174
R^a	0.018	0.029	0.028
R_w	0.026	0.036	0.029
R_{all}	0.032	0.039	0.095
GOF	1.11	1.36	0.91
max Δ/σ in final cycle	0.11	0.00	0.00

[a] $R = \sum||F_o| - |F_c||/\sum|F_o|$.

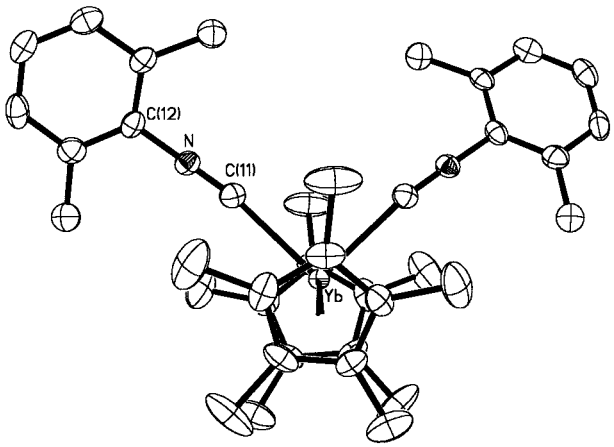

Figure 4. ORTEP diagram of $(Me_5C_5)_2Yb(2,6\text{-}Me_2C_6H_3NC)_2$ (50% probability ellipsoids).

Downloaded by CARLI CONSORTIUM on June 29, 2009
Published on November 27, 2001 on http://pubs.acs.org | doi: 10.1021/om0106579

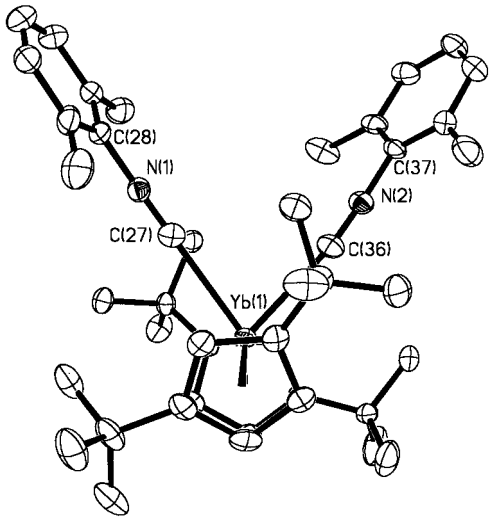

Figure 5. ORTEP diagram of $[1,3\text{-}(Me_3C)_2C_5H_3]_2Yb(2,6\text{-}Me_2C_6H_3NC)_2$ (50% probability ellipsoids).

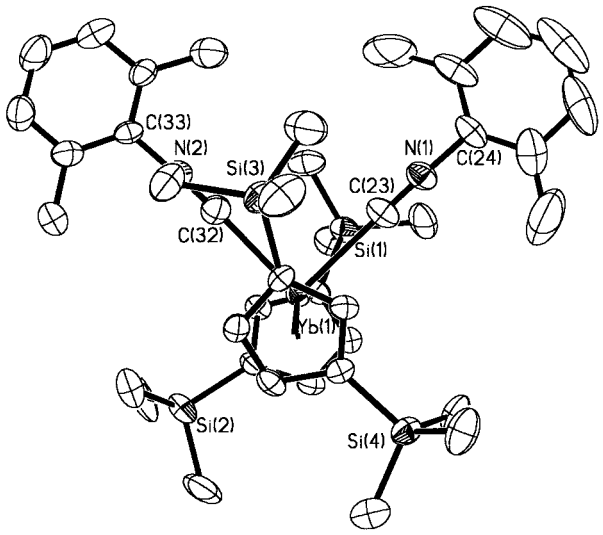

Figure 6. ORTEP diagram of $[1,3\text{-}(Me_3Si)_2C_5H_3]_2Yb(2,6\text{-}Me_2C_6H_3NC)_2$ (50% probability ellipsoids).

staggered in the Me_3Si case. In addition, the xylyl rings of the isocyanide ligands lie in different orientations for these two molecules; in the Me_3C case, they are perpendicular to the plane bisecting the metallocene wedge, while in the Me_3Si case they lie in that plane. This is presumably due to the steric demands of the Me_3C groups on the cyclopentadienide rings, which avoid each other to the greatest possible degree when the rings are eclipsed. The two xylyl rings tilt to minimize steric repulsions with the Me_3C groups, and the resulting isocyanide $C_{CNR}-Yb-C_{CNR}$ angle is 80°. In the Me_3Si derivative, the isocyanide $C_{CNR}-Yb-C_{CNR}$ angle is 10° larger than in the Me_3C derivative, and the xylyl rings lie in the same plane. All of the $C_{CNR}-N$ distances are very close to that of the free ligand $2,6\text{-}Me_2C_6H_3NC$ (1.16 Å). The centroid−metal−centroid angles of the three complexes are smaller than in the base-free complexes.[15,16] This is an expected consequence of the addition of two ligands to the coordination sphere of the metal; the distances and angles are similar to those found for other complexes of the type Cp'_2YbL_2.[30,31]

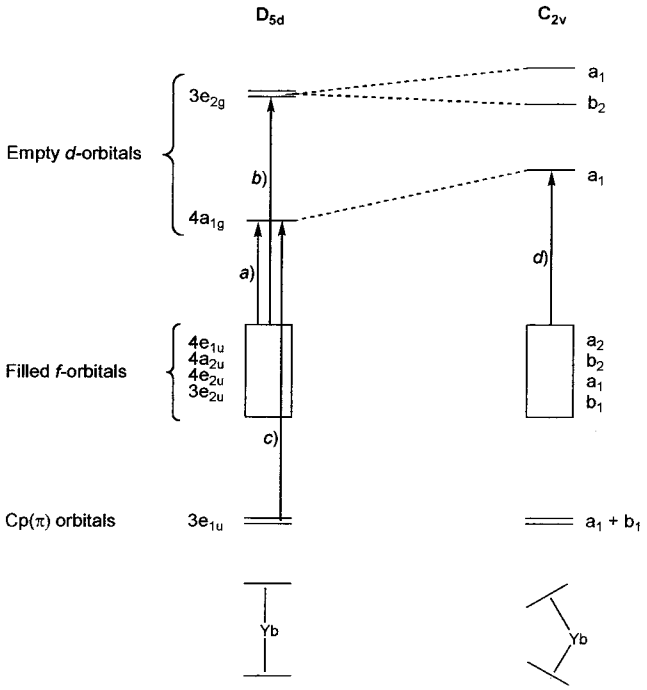

Figure 7. Schematic energy diagram showing the effect of bending on the energies of the molecular orbitals and the optical transitions of an ytterbocene. The diagram is constructed from the data in ref 13 but is not to scale. The transitions depicted are as follows: (*a*) HOMO → LUMO, $4e_{1u} \rightarrow 4a_{1g}$; (*b*) f → d, $4e_{2u} \rightarrow 3e_{2g}$; (*c*) LMCT, $3e_{1u} \rightarrow 4a_{1g}$; (*d*) HOMO → LUMO, f → a_1.

Discussion

UV Spectroscopy. The absorptions observed in the optical spectra of the base-free ytterbocenes and their adducts from 1000 to 350 nm are listed in Table 2. The assignment of the transitions for $(Me_5C_5)_2Yb$ is based upon the calculated transition energies of $(C_5H_5)_2Yb$ in D_{5d} symmetry, since the ground-state energy does not change much on bending to C_{2v} symmetry.[13,32] Three transitions in this energy range are predicted. The highest wavelength transition is the HOMO → LUMO ($e_{1u} \rightarrow a_{1g}$ orbitals in D_{5d} symmetry) (Figure 7). The e_{1u} symmetry orbital is exclusively an f orbital in D_{5d} symmetry, and this transition, which is predicted to occur at about 750 nm, is responsible for the color of the ytterbocene. The next lower wavelength transitions are predicted to occur at about 460 and 390 nm, due to the Cp(π) → LUMO ($e_{1u} \rightarrow a_{1g}$, LMCT) and the f → d ($e_{2u} \rightarrow e_{2g}$) transition, respectively.[13] All of these transitions, in D_{5d} symmetry, are electric dipole and Laporte allowed; therefore, they are expected to have large absorptivities, as observed. The first- and third-mentioned absorptions involve transitions between f and d orbitals, which do not mix in D_{5d} symmetry. As the metallocenes bend and the symmetry is lowered to C_{2v}, mixing of the f and d orbitals occurs; however, the transitions are still electric dipole allowed (Figure 7).

In methylcyclohexane, the HOMO−LUMO transition of $(Me_5C_5)_2Yb$ is assigned to the feature at 751 nm. The

(30) Tilley, T. D.; Andersen, R. A.; Spencer, B.; Zalkin, A. *Inorg. Chem.* **1982**, *21*, 2647−2649.
(31) Tilley, T. D.; Andersen, R. A.; Spencer, B.; Ruben, H.; Zalkin, A.; Templeton, D. H. *Inorg. Chem.* **1980**, *19*, 2999−3003.
(32) DeKock, R. L.; Peterson, M. A.; Timmer, L. K.; Baerends, E. J.; Vernooijs, P. *Polyhedron* **1990**, *9*, 1919−1934.

Downloaded by CARLI CONSORTIUM on June 29, 2009
Published on November 27, 2001 on http://pubs.acs.org | doi: 10.1021/om0106579

Downloaded by CARLI CONSORTIUM on June 29, 2009
Published on November 27, 2001 on http://pubs.acs.org | doi: 10.1021/om0106579

lower wavelength transitions at 515, 474, and 429 nm are assigned to transitions from the lower lying filled molecular orbitals. Three rather than two absorptions are observed, possibly due to the reduction in symmetry from D_{5d} to C_{2v}, which removes the orbital degeneracies. The average observed energy of these three bands is 473 nm, close to the average calculated value of 425 nm for $(C_5H_5)_2Yb$; therefore, the predicted transition energies are in good agreement with the observed values.

The principal change that is predicted to occur on bending $(C_5H_5)_2Yb$, and presumably $(Me_5C_5)_2Yb$, from D_{5d} to C_{2v} symmetry is an increase in the HOMO−LUMO gap.[13] Thus, bending is predicted to result in a blue shift of the HOMO−LUMO transition. The increased HOMO−LUMO gap that results from bending is largely due to destabilization of the lowest energy, empty a_1 symmetry orbital (in C_{2v} symmetry; a_{1g} in D_{5d}), while the next two higher energy orbitals (a_1 and b_2 in C_{2v}, e_{2g} in D_{5d}) change little on bending (Figure 7). It is therefore tempting to offer this as an explanation for the blue shift of 14 nm in the HOMO−LUMO transition on changing the solvent from methylcyclohexane to toluene. If correct, this implies that the average geometry of the ytterbocene is more bent in aromatic solvents than in aliphatic ones, which seems reasonable, as toluene is a better electron donor than its saturated analogue.

The electronic transitions of $[1,3\text{-}(Me_3C)_2C_5H_3]_2Yb$ and $[1,3\text{-}(Me_3Si)_2C_5H_3]_2Yb$ in methylcyclohexane are given in Table 2. The highest wavelength transitions in these spectra, at 655 and 648 nm, respectively, can be assigned to the HOMO−LUMO transition using the Rösch−Green model.[13] The transitions in these two metallocenes are blue shifted by about 100 nm (2000 cm^{-1}) relative to $(Me_5C_5)_2Yb$. In addition, the average value of the lower wavelength absorptions is nearly identical, 430 nm, with the average in $(Me_5C_5)_2Yb$, 473 nm. The similarity of the transitions in the two disubstituted ytterbocenes is surprising, since the steric and electronic effects of Me_3C and Me_3Si are quite different; Me_3C has a larger cone angle and is a better donor than Me_3Si. Also, the values of ν_{CO} for the carbonyl complexes previously discussed lie in the order $Me_3Si > Me_3C$, which supports the idea that Me_3C is more donating (Table 1). One explanation is that the molecules have similar sandwich structures in methylcyclohexane, which are more bent than $(Me_5C_5)_2Yb$. This accounts for the nearly identical energies of their HOMO−LUMO transitions in solution. It also accounts for the purple solid $[1,3\text{-}(Me_3Si)_2C_5H_3]_2Yb$ (centroid−metal−centroid angle 138°[16]) becoming olive brown when it is dissolved in methylcyclohexane. The red shift results when the bend angle becomes larger in solution, as the molecule is no longer constrained by the intermolecular interactions of the solid state.

The HOMO−LUMO transition of $(Me_5C_5)_2Yb$ in methylcyclohexane shifts to 699 nm when it is exposed to CO, a blue shift of 52 nm. The lower wavelength transitions shift less than 5 nm. When a 1:1 or 1:2 adduct of a metallocene forms, the resulting angle of the bent sandwich is smaller than in the base-free complex. Electronically, the donor ligands interact with the empty a_1 and b_2 (C_{2v} symmetry) orbitals, stabilizing the filled bonding orbitals and destabilizing the empty antibonding ones. The net result of adduct formation is therefore to raise the LUMO orbital in energy. However, the filled orbitals, including the HOMO, are also increased in energy, since adding electron density raises their energy. This destabilization can be thought of as arising from the electron−electron repulsion within the f orbitals in the closed-shell $4f^{14}$ Yb(II). Thus, the net effect on the HOMO−LUMO transition of adduct formation could be either a blue or a red shift, depending on the extent of bending and the extent of electron donation from the ligands. In the $(Me_5C_5)_2Yb$ and CO system, the blue shift of 52 nm (1000 cm^{-1}) in methylcyclohexane is presumably due mainly to bending, which raises the LUMO more than the HOMO, as the interaction with the ligand is expected to be small. In the adduct $(Me_5C_5)_2Yb(OEt_2)$ in toluene, the HOMO−LUMO transition is similarly blue shifted by 66 nm relative to base-free $(Me_5C_5)_2Yb$ in toluene.[33,34]

The model developed above can be extended to the isocyanide adducts. In those complexes, the low-energy band that is a measure of the HOMO−LUMO gap changes significantly, depending on the substituents on the cyclopentadienide ring and on the isocyanide ligand. In crystalline $(Me_5C_5)_2Yb(2,6\text{-}Me_2C_6H_3NC)_2$, the bend angle of 145° is similar to that found in the 1:1 THF adduct,[31] and the HOMO−LUMO transition in solution (776 nm) is also similar to that of the THF adduct (790 nm).[34] Replacing the xylyl group with the more strongly donating alkyl groups on the isocyanides results in a red shift of the HOMO−LUMO transition (Table 2), which indicates that the HOMO−LUMO gap is decreasing. This effect is presumably the result of the higher electron density of the alkyl isocyanide ligands increasing the energy of the HOMO by electron−electron repulsion. Changing the substituents on the cyclopentadienide ring to $(Me_3C)_2$ and $(Me_3Si)_2$ decreases the centroid−metal−centroid angles of the isocyanide complexes in the solid state relative to $(Me_5C_5)_2Yb(2,6\text{-}Me_2C_6H_3NC)_2$, and the HOMO−LUMO transitions for the xylyl isocyanide adducts in toluene solution are blue-shifted to 586 and 617 nm, respectively, consistent with a greater degree of bending in solution. For those ytterbocenes, the alkyl isocyanide complexes are also red-shifted from the xylyl isocyanide complexes. The ytterbocene $(Me_4C_5H)_2Yb$ appears to be very similar to $(Me_5C_5)_2Yb$, on the basis of the optical spectra of its isocyanide complexes.

Infrared and NMR Spectroscopy. The infrared spectrum of a methylcyclohexane solution of $(Me_5C_5)_2Yb$ under CO clearly shows two CO stretches (Figure 1). Both ν_{CO} values are lower than that of free CO, consistent with population of the C−O π-antibonding orbital by metal → ligand donation. In a detailed study of the pressure and temperature dependence of these two absorptions, the 2114 cm^{-1} band is attributed to a monocarbonyl species and the 2072 cm^{-1} band to a dicarbonyl species.[21] The latter band is clearly broader and less intense than the former (Figure 1), possibly due to unresolved, small coupling between the two carbonyl groups in C_{2v} symmetry.[35] The explanation

(33) Thomas, A. C.; Ellis, A. B. *Organometallics* **1985**, *4*, 2223−2225.
(34) Thomas, A. C. Ph.D. Thesis, University of Wisconsin−Madison, Madison, WI, 1985.
(35) Willner, H.; Aubke, F. *Angew. Chem., Int. Ed.* **1997**, *36*, 2402−2425.

Downloaded by CARLI CONSORTIUM on June 29, 2009
Published on November 27, 2001 on http://pubs.acs.org | doi: 10.1021/om0106579

that two carbonyl species are in equilibrium is supported by the variable-temperature ^{13}C NMR spectra of a $(Me_5C_5)_2Yb$ solution under 1 atm of ^{13}CO. At room temperature, only a single ^{13}CO resonance is observed at δ 203 ppm ($\nu_{1/2} = 425$ Hz), which is deshielded by 18 ppm relative to free ^{13}CO at the same temperature and pressure. The single averaged resonance decoalesces into two at −107 °C at δ 243 ppm ($\nu_{1/2} = 2800$ Hz) and δ 199 ppm ($\nu_{1/2} = 100$ Hz), both of which are deshielded relative to free ^{13}CO. The corresponding proton NMR spectra are unchanged from that of a $(Me_5C_5)_2Yb$ solution in the absence of CO.

The ^{13}C chemical shift in a carbonyl complex, δ_{CO}, is directly related to the nuclear magnetic shielding, $-\sigma$. Thus, as $-\sigma$ decreases the nucleus is deshielded, giving a resonance at higher frequency corresponding to a downfield chemical shift. Conversely, a less negative value of $-\sigma$ results in an upfield shift.[36,37] The origin of ^{13}C chemical shifts in diamagnetic molecules using Ramsey's model is $\sigma_{total} = \sigma_{diamagnetic} + \sigma_{paramagnetic}$, and the paramagnetic component is the dominant term. This term is proportional to the reciprocal of the excitation energy multiplied by the distance cubed, $\Delta E^{-1} r^{-3}$. Accordingly, the closer the ^{13}C nucleus in question is to the electrons around the metal, the greater the paramagnetic term will be, and this larger negative shielding results in a downfield chemical shift. It is therefore axiomatic that the ^{13}C chemical shift is correlated with the CO stretching frequency in the infrared spectrum; π-back-bonding increases the electron density in the metal−carbon bond, shortening it and deshielding the ^{13}C resonance, while simultaneously lengthening the C−O bond and reducing the CO stretching frequency. The converse is also true; therefore, a shielded ^{13}C resonance is expected when ν_{CO} moves to a higher frequency. This correlation has been graphically illustrated for d^0 metallocene carbonyl complexes by Parkin.[38] Thus, $(Me_5C_5)_2HfH_2(CO)$ at room temperature has δ_{CO} at 224 ppm and ν_{CO} at 2036 cm^{-1}.[39] Conversely, for $(Me_5C_5)_2Ca(CO)$ in toluene, the averaged chemical shift is shielded (δ_{CO} 180.4 ppm) and ν_{CO} is raised (2158 cm^{-1}) with respect to free CO.[23]

An electrostatic bonding model has been advanced to explain the increase in CO stretching frequency above that of free CO in some metal carbonyl compounds.[35,40−42] In this model, when the carbon atom of CO is located near an electropositive metal atom, the polarization in the CO ligand changes as shown in the valence diagram **A**. The orbital energy of the carbon atom becomes closer to that of the oxygen atom, making the bond more covalent. Hence, the force constant of the C−O bond increases, ν_{CO} increases, and δ_{CO} is shielded. In cases where ν_{CO} is reduced, π-back-bonding from the metal fragment competes with or dominates the electrostatic interaction and δ_{CO} is deshielded. The resulting charge distribution is illustrated by the valence bond picture **B**. Thus, the variation of ν_{CO} observed in the three ytterbocene molecules examined here, from slightly higher than that of free CO to somewhat lower, is an indication of the balance between the resonance forms **A** and **B**.

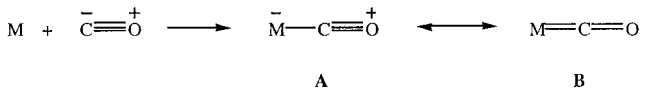

A **B**

The isocyanide complexes of the ytterbocenes are isolable 1:2 adducts which are therefore structural models for the postulated dicarbonyl adduct of $(Me_5C_5)_2Yb$. Structurally, the only notable difference between the three ytterbocene xylyl isocyanide complexes is the orientation of the disubstituted rings and the isocyanide ligands of those complexes as described above. The solid-state structure is not maintained in solution, since the adducts undergo fast intermolecular exchange on the NMR time scale, as expected for ytterbocene adducts.[17,18]

Even though 1:2 isocyanide adducts are isolated in the solid state, only a single, sharp CN stretching frequency is observed in the solid state (Nujol) or solution infrared spectra. In addition, the values of ν_{CN} in all of the adducts is greater than those found in the free isocyanides by 11−35 cm^{-1}. The electrostatic model, persuasively argued by Berke for borane adducts of isocyanides,[43,44] can be applied to these isocyanide complexes in a manner analogous to that for the carbonyl complexes just described. When an isocyanide is placed near a positive charge, the negative charge on the carbon atom is reduced. This lowers the atomic orbital energy of the carbon atom, bringing it closer in energy to the NR fragment. The net effect is to shorten and strengthen the C−N bond, resulting in an increase in ν_{CNR}. This is illustrated by the valence bond structure **C**, in which the charge distribution is similar to that in the CO complexes described above.

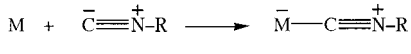

C

This model should be particularly applicable to the isocyanide adducts described here, since the bonding in lanthanide compounds is largely electrostatic in nature. The interaction of an isocyanide ligand with a bivalent metal is expected to be weaker than with a trivalent metal in the electrostatic bonding model because of the smaller charge in the former. Consistent with this argument, the increase in ν_{CN} in the trivalent complexes $(C_5H_5)_3Ln(C_6H_{11}NC)$ of 60−74 cm^{-1} is greater than that observed for the bivalent complexes described here of 11−35 cm^{-1}.[27,28] In addition, the electrostatic model implies that when two isocyanide ligands are present in the same molecule they will behave as independent dipoles, giving rise to a single ν_{CN} stretch, in accord with the observed data (Table 1).

(36) Mason, J. *Multinuclear NMR*; Plenum Press: New York, 1987; Chapter 3.
(37) Ehlers, A. W.; Ruiz-Morales, Y.; Baerends, E. J.; Ziegler, T. *Inorg. Chem*. **1997**, *36*, 5031−5036.
(38) Howard, W. A.; Parkin, G. F. R.; Rheingold, A. L. *Polyhedron* **1995**, *14*, 25−44.
(39) Roddick, D. M.; Fryzuk, M. D.; Seidler, P. F.; Hillhouse, G. L.; Bercaw, J. E. *Organometallics* **1985**, *4*, 97−104.
(40) Goldman, A. S.; Krogh-Jesperson, K. *J. Am. Chem. Soc.* **1996**, *118*, 12159−12166.
(41) Hush, N. S.; Williams, M. L. *J. Mol. Spectrosc.* **1974**, *50*, 349−368.
(42) Strauss, S. H. *Chemtracts-Inorg. Chem*. **1997**, *10*, 77−103.
(43) Jacobsen, H.; Berke, H.; Döring, S.; Kehr, G.; Erker, G.; Fröhlich, R.; Meyer, O. *Organometallics* **1999**, *18*, 1724−1735.
(44) Stauch, H. C.; Wibbeling, B.; Fröhlich, R.; Erker, G.; Jacobsen, H.; Berke, H. *Organometallics* **1999**, *18*, 3802−3812.

Downloaded by CARLI CONSORTIUM on June 29, 2009
Published on November 27, 2001 on http://pubs.acs.org | doi: 10.1021/om0106579

Epilogue

Bis(pentamethylcyclopentadienyl)ytterbium is a rather special metallocene. In solution, it coordinates up to two carbon monoxide ligands, and the infrared stretching frequency and ^{13}C NMR chemical shifts of the carbonyl complexes indicate that the bivalent lanthanide metallocene is acting as a π-base. Thus, it has certain similarities with the lower valent d-transition-metal metallocenes. As it is a bent sandwich, the electrons in the 5d orbitals can mix with the 4f electrons, and it is our view that this mixing is the reason for the π-basicity toward CO, since the ligand (crystal) field effects are greater for d than for f electrons, increasing the importance of their role in π-back-bonding. The other two ytterbocenes described here each have a single CO stretch in their infrared spectra upon exposure to CO, the values of which show that $(Me_5C_5)_2Yb$ is a substantially better donor fragment, as is expected from the more electron-rich cyclopentadienide rings in $(Me_5C_5)_2Yb$.

One important message from our results is that, in contrast to the generalization commonly found in textbooks, the physical and chemical properties of bivalent lanthanide metals and alkaline-earth metals are not the same. When $(Me_5C_5)_2Yb$ is compared with $(Me_5C_5)_2Ca$, the metal radii are nearly identical,[24] as are the structures of the metallocenes in the solid state and gas phase.[15,45] Both coordinate carbon monoxide in solution, but the values of ν_{CO} and δ_{CO} for the ytterbium carbonyls, with electronic structure $5d^0\ 4f^{14}$, show that the C−O bond force constant is lowered relative to free CO. In contrast, the values of ν_{CO} and δ_{CO} for the calcium fragment, with electronic structure $3d^0\ 3p^6$, show that the C−O force constant increases in that case. Thus, this bivalent ytterbocene does participate in back-donation, whereas the calcium analogue does not.

Experimental Section

General Comments. All reactions and product manipulations were carried out under dry nitrogen using standard Schlenk and drybox techniques. Dry, oxygen-free solvents were employed throughout. The elemental analyses were performed by the analytical facility at the University of California at Berkeley. The ^{13}C NMR spectra were collected at 75 MHz for the isotopically labeled ^{13}CO experiments. The following ytterbocene compounds were prepared as previously described: $(Me_5C_5)_2Yb(OEt_2)$,,[46] $(Me_5C_5)_2Yb$,[15] $[1,3\text{-}(Me_3C)_2C_5H_3]_2Yb(OEt_2)$,[15] $[1,3\text{-}(Me_3C)_2C_5H_3]_2Yb$,[15] $[1,3\text{-}(Me_3Si)_2C_5H_3]_2Yb(OEt_2)$,[16] $[1,3\text{-}(Me_3Si)_2C_5H_3]_2Yb$,[16] $(Me_4C_5H)_2Yb(OEt_2)$,[15] $(Me_4C_5H)_2Yb$.[15] The isocyanide ligands were purified by sublimation ($2,6\text{-}Me_2C_6H_3NC$) or distillation (Me_3CNC, $C_6H_{11}NC$).

Infrared Spectroscopy. The infrared spectra for solid samples were recorded as Nujol mulls on a Mattson Nicolet instrument. Solution infrared spectra were recorded using an ASI ReactIR instrument with a Cajon adapter to a modified Schlenk flask. A background spectrum was collected on the contents of the flask under a nitrogen atmosphere. Spectra of the solvent and solvent with solute were then collected. The last two spectra were subtracted using an interactive procedure to achieve as flat a baseline as possible to give the spectrum of the compound. For carbonyl complexes, the flask was then exposed briefly to vacuum and back-filled with carbon monoxide (99.99% purity), and a third spectrum was recorded. The spectrum of the carbonyl complex was obtained by subtracting the spectrum of the solute from the spectrum of the solute in the presence of the gas. Only the ν_{CO} or ν_{CN} frequencies are reported in Table 1.

$(Me_5C_5)_2Yb(2,6\text{-}Me_2C_6H_3NC)_2$. A toluene solution (10 mL) of $(Me_5C_5)_2Yb(OEt_2)$ (0.14 g, 0.32 mmol) was added with stirring to a toluene solution (5 mL) of $2,6\text{-}Me_2C_6H_3NC$ (0.080 g, 0.61 mmol). Reduction of the volume of solvent to 5 mL and cooling to −25 °C led to the formation of brown-green blocks. A second batch of crystals was isolated from the mother liquors by concentrating and cooling. Yield: 0.18 g (84%). Mp: 199−202 °C. Anal. Calcd for $C_{38}H_{48}N_2Yb$: C, 64.7; H, 6.85; N, 3.97. Found: C, 65.0; H, 6.71; N, 3.98. ^1H NMR (C_6D_6): δ 6.90 (t, J = 8 Hz, 2H, C_6H_3), 6.55 (d, J = 8 Hz, 4H, C_6H_3), 2.36 (s, 30H, Me_5), 2.07 (s, 12 H, Me_2) ppm. ^{13}C NMR (C_6D_6): δ 134.0 (N−*C*), 129.2, 128.8, 128.5 (phenyl C's), 111.3 (C_5), 19.0 (Me_2), 11.7 (Me_5) ppm (*C*≡N not observed).

$(Me_5C_5)_2Yb(Me_3CNC)_2\cdot$(toluene). A procedure similar to that used to prepare $(Me_5C_5)_2Yb(2,6\text{-}Me_2C_6H_3NC)_2$ was followed, yielding bright red crystals which contain one molecule of toluene of crystallization per metal atom. Yield: 80%. Mp: 105−109 °C. Anal. Calcd for $C_{37}H_{56}N_2Yb$: C, 63.3; H, 8.04; N, 3.99. Found: C, 64.1; H, 8.16; N, 3.96. ^1H NMR (C_6D_6): δ 7.05 (m, 5H, tol), 2.33 (s, 30H, Me_5), 2.11 (s, 3H, tol), 1.01 (br s, 18 H, Me_3) ppm.

$(Me_5C_5)_2Yb(C_6H_{11}NC)_2$. A procedure similar to that used to prepare $(Me_5C_5)_2Yb(2,6\text{-}Me_2C_6H_3NC)_2$ was followed, yielding bright red crystals. Yield: 70%. Mp: 175−178 °C. Anal. Calcd for $C_{34}H_{52}N_2Yb$: C, 61.7; H, 7.92; N, 4.23. Found: C, 62.1; H, 7.97; N, 4.25. ^1H NMR (C_6D_6): δ 2.55 (br s, 2H, C_6H_{11}), 2.39 (s, 30H, Me_5), 1.35 (br s, 12H, C_6H_{11}), 0.81 (br s, 8H, C_6H_{11}) ppm.

$[1,3\text{-}(Me_3C)_2C_5H_3]_2Yb(2,6\text{-}Me_2C_6H_3NC)_2$. In a nitrogen-containing glovebox, $[1,3\text{-}(Me_3C)_2C_5H_3]_2Yb(OEt_2)$ (0.58 g, 0.97 mmol) and $2,6\text{-}Me_2C_6H_3NC$ (0.25 g, 1.94 mmol) were placed in a Schlenk flask. Toluene (30 mL) was added, the dark solution was briefly stirred, and the volume of solvent was reduced to 10 mL. Cooling to −40 °C resulted in the formation of deep blue crystals. Yield: 0.6 g (85%). Mp: 163−166 °C. Anal. Calcd for $C_{44}H_{60}N_2Yb$: C, 66.9; H, 7.66; N, 3.55. Found: C, 66.7; H, 7.76; N, 3.40. ^1H NMR (tol-d_8): δ 6.77 (t, J = 7.7 Hz, 2H, C_6H_3), 6.56 (d, J = 7.6 Hz, 4H, C_6H_3), 6.14 (d, J = 2.5 Hz, 4H, C_5H_3), 6.10 (t, J = 2.4 Hz, 2H, C_5H_3), 2.12 (s, 12H, Me_2), 1.42 (s, 36H, Me_3C) ppm.

$[1,3\text{-}(Me_3C)_2C_5H_3]_2Yb(Me_3CNC)_2$. Under a flow of nitrogen, $[1,3\text{-}(Me_3C)_2C_5H_3]_2Yb(OEt_2)$ (0.73 g, 1.2 mmol) was weighed into a Schlenk flask. Toluene (30 mL) was added, followed by Me_3CNC (0.20 g, 0.275 mL, 2.4 mmol), and the solution was stirred briefly. The volume of the blood red solution was reduced to 25 mL, and then it was cooled to −40 °C to give deep red crystals. Yield: 0.7 g (85%). Mp: 165−169 °C. Anal. Calcd for $C_{36}H_{60}N_2Yb$: C, 62.3; H, 8.72; N, 4.04. Found: C, 63.4; H, 9.2; N, 4.08. ^1H NMR (tol-d_8): δ 6.03 (br, 4H, C_5H_3), 5.98 (br, 2H, C_5H_3), 1.46 (s, 36H, ring Me_3C), 0.98 (s, 18H, isocyanide Me_3C) ppm.

$[1,3\text{-}(Me_3C)_2C_5H_3]_2Yb(C_6H_{11}NC)_2$. A procedure similar to that used to prepare $[1,3\text{-}(Me_3C)_2C_5H_3]_2Yb(Me_3CNC)_2$ was followed, yielding brick red crystals. Yield: 89%. Mp: 148−150 °C. Anal. Calcd for $C_{40}H_{62}N_2Yb$: C, 64.4; H, 8.65; N, 3.76. Found: C, 63.0; H, 8.64; N, 3.56. ^1H NMR (tol-d_8): δ 6.18 (br, 4H, C_5H_3), 6.14 (br, 2H, C_5H_3), 2.79 (br, 2H, C_6H_{11}), 1.56 (s, 36 H, Me_3C), 1.36 (br, 12H, C_6H_{11}), 1.00 (br m, 8H, C_6H_{11}) ppm.

$[1,3\text{-}(Me_3Si)_2C_5H_3]_2Yb(2,6\text{-}Me_2C_6H_3NC)_2$. A procedure similar to that used to prepare $[1,3\text{-}(Me_3C)_2C_5H_3]_2Yb(2,6\text{-}Me_2C_6H_3\text{-}NC)_2$ gave dark blue crystals. Yield: 90%. Mp: 155−158 °C. Anal. Calcd for $C_{40}H_{60}Si_4N_2Yb$: C, 56.2; H, 7.08; N, 3.28. Found: C, 54.6; H, 6.64; N, 2.74. ^1H NMR (C_6D_6): δ 6.80 (br m, 12H, C_5H_3 and C_6H_3), 2.45 (br s, 12H, Me_2), 0.47 (s, 36H, Me_3Si) ppm.

(45) Andersen, R. A.; Boncella, J. M.; Burns, C. J.; Blom, R.; Haaland, A.; Volden, H. V. *J. Organomet. Chem.* **1986**, *312*, C49−C52.
(46) Tilley, T. D.; Boncella, J. M.; Berg, D. J.; Burns, C. J.; Andersen, R. A. *Inorg. Synth.* **1990**, *27*, 146−149.

Downloaded by CARLI CONSORTIUM on June 29, 2009
Published on November 27, 2001 on http://pubs.acs.org | doi: 10.1021/om0106579

$[1,3\text{-}(Me_3Si)_2C_5H_3]_2Yb(C_6H_{11}NC)_2$. A procedure similar to that used to prepare $[1,3\text{-}(Me_3C)_2C_5H_3]_2Yb(Me_3CNC)_2$ was followed, yielding brick red crystals. Yield: 85%. Mp: 142−144 °C. Anal. Calcd for $C_{36}H_{64}Si_4N_2Yb$: C, 53.4; H, 7.96; N, 3.46. Found: C, 53.0; H, 8.13; N, 3.40. ^{1}H NMR (C_6D_6): δ 6.72 (br, 4H, C_5H_3), 6.69 (br, 2H, C_5H_3), 2.90 (br s, 2H, C_6H_{11}), 1.48 (br s, 4H, C_6H_{11}), 1.37 (br s, 8H, C_6H_{11}), 0.93 (br m, 8H, C_6H_{11}), 0.50 (s, 36H, Me_3Si) ppm.

$(Me_4C_5H)_2Yb(2,6\text{-}Me_2C_6H_3NC)_2$. A procedure similar to that used to prepare $[1,3\text{-}(Me_3C)_2C_5H_3]_2Yb(2,6\text{-}Me_2C_6H_3NC)_2$ was followed, and dark blue-green crystals were isolated in 70% yield. Mp: 180−182 °C. Anal. Calcd for $C_{36}H_{44}N_2Yb$: C, 63.8; H, 6.54; N, 4.13. Found: C, 63.5; H, 6.34; N, 3.88. ^{1}H NMR (C_6D_6): δ 6.93 (t, $J = 7$ Hz, 2H, C_6H_3), 6.52 (d, $J = 7$ Hz, 4H, C_6H_3), 5.88 (s, 2H, C_5H), 2.44 (s, 12H, Me_4C_5), 2.39 (s, 12H, Me_4C_5), 2.03 (s, 12H, Me_2) ppm.

$(Me_4C_5H)_2Yb(Me_3CNC)_2$. A procedure similar to that used to prepare $[1,3\text{-}(Me_3C)_2C_5H_3]_2Yb(Me_3CNC)_2$ was followed, and the product was isolated as red crystals in 80% yield. Mp: 105−108 °C. Anal. Calcd for $C_{28}H_{44}N_2Yb$: C, 57.8; H, 7.62; N, 4.82. Found: C, 58.7; H, 7.40; N, 4.29. ^{1}H NMR (C_6D_6): δ 5.9 (s, 2H, C_5H), 1.79 (s, 12H, Me_4C_5), 1.75 (s, 12H, Me_4C_5) ppm (Me_3CNC resonances not observed).

$(Me_4C_5H)_2Yb(C_6H_{11}NC)_2$. A procedure similar to that used to prepare $[1,3\text{-}(Me_3C)_2C_5H_3]_2Yb(Me_3CNC)_2$ was followed, and the product was isolated as red crystals in 90% yield. Mp: 136−139 °C. Anal. Calcd for $C_{32}H_{48}N_2Yb$: C, 60.6; H, 7.63; N, 4.42. Found: C, 60.6; H, 7.43; N, 4.16. ^{1}H NMR (C_6D_6): δ 5.89 (s, 2H, C_5H), 2.63 (s, 2H, C_6H_{11}), 2.47 (s, 12H, Me_4C_5), 2.40 (s, 12H, Me_4C_5), 1.3 (br m, 12 H, C_6H_{11}), 0.8 (br m, 8 H, C_6H_{11}) ppm.

Crystallographic Studies. General Procedure. All relevant crystallographic data are shown in Table 4. For each complex studied by X-ray diffraction, crystals were grown by slow cooling of a concentrated toluene solution of the compound. A crystal was mounted on a glass fiber with Paratone N hydrocarbon oil. All measurements were made on a Siemens SMART[47] diffractometer with graphite-monochromated Mo Kα radiation using a CCD detector. Cell constants and an orientation matrix for data collection were obtained from a least-squares refinement of reflections from 60 frames collected at 10 s each. Frames corresponding to a hemisphere of data were then collected using the ω-scan technique; in each case 10 s exposures of 0.3° in ω were taken. The reflections were integrated using SAINT,[48] and equivalent reflections were merged. No decay correction was applied. An empirical absorption correction was applied to each structure as described below, and the data were corrected for Lorentz and polarization effects. The space groups were determined by the systematic absences of *hkl* values, unless otherwise noted. The structures were solved by direct methods[49] and expanded using Fourier techniques. All non-hydrogen atoms were refined anisotropically; hydrogen atoms were included but not refined unless otherwise noted. The final cycle of full-matrix least-squares refinement was based on observed reflections ($I > 3.00\sigma(I)$) and converged. The function minimized was $\sum w(|F_o| - |F_c|)^2$. The weighting scheme was based on counting statistics and included a factor ($p = 0.030$) to downweight intense reflections. Plots of $\sum w(|F_o| - |F_c|)^2$ vs $|F_o|$, reflection order in data collection, $(\sin\theta)/\lambda$, and various classes of indices showed no unusual trends. Neutral atom scattering factors were taken from ref 50. Anomalous dispersion effects were included in F_c; the values for $\Delta f'$ and $\Delta f''$ were those of Creagh and McAuley.[51] The values for the mass attenuation coefficients are those of Creagh and Hubbell.[52] All calculations were performed using the teXsan crystallographic software package of Molecular Structure Corp.[53]

$(Me_5C_5)_2Yb(2,6\text{-}Me_2C_6H_3NC)_2$. An empirical absorption correction was applied using XPREP[54] with $\mu R = 0.06$. A secondary extinction coefficient was applied (1.4×10^{-7}). The quality of the data indicated that it was reasonable to locate and refine hydrogen atoms.

$[1,3\text{-}(Me_3C)_2C_5H_3]_2Yb(2,6\text{-}Me_2C_6H_3NC)_2$. On the basis of a statistical analysis of intensity distribution, and the successful solution and refinement of the structure, the space group was determined to be $P\bar{1}$ (No. 2). An empirical absorption correction was applied using XPREP[54] with $\mu R = 0.03$. Analysis of the data indicated no need for a secondary extinction correction.

$[1,3\text{-}(Me_3Si)_2C_5H_3]_2Yb(2,6\text{-}Me_2C_6H_3NC)_2$. An empirical absorption correction was applied using SADABS.[55] No secondary extinction correction was applied.

Acknowledgment. This work was partially supported by the Director, Office of Energy Research, Office of Basic Energy Sciences, Chemical Sciences Division of the U.S. Department of Energy under Contract No. DE-AC03-76SF00098. We thank the Fannie and John Hertz Foundation for a fellowship (C.J.B.), the NSF for a fellowship (D.J.S.), and Dr. Fred Hollander for assistance with the crystallography. We also thank Professor Art Ellis for making A. C. Thomas' Ph.D. thesis available and Dr. Wayne Lukens and Professor Hans Brintzinger for helpful discussion.

Note Added in Proof. DFT calculations on the carbon monoxide adducts are underway, O. Eisenstein and L. Maron, personal communication.

Supporting Information Available: Tables giving atomic positions, anisotropic thermal parameters, bond lengths and angles, and least-squares planes for each structure. This material is available free of charge via the Internet at http://pubs.acs.org. Structure factor tables are available from the authors.

OM0106579

(47) SMART Area-Detection Software Package; Siemens Industrial Automation, Inc., Madison, WI, 1995.
(48) SAINT, version 4.024; Siemens Industrial Automation, Inc., Madison, WI, 1995.
(49) Altomare, A.; Cascarano, M.; Giacovazzo, C.; Guagliardi, A. *J. Appl. Crystallogr.* **1993**, *26*, 343−350.
(50) Cromer, D. T.; Waber, J. T. In *International Tables for X-ray Crystallography*; Ibers, J. A., Hamilton, W. C., Eds.; Kynoch Press: Birmingham, England, 1974; Vol. IV, Table 2.2A, pp 71−98.
(51) Creagh, D. C.; McAuley, W. J. In *International Tables for Crystallography*; Wilson, A. J. C., Ed.; Kluwer Academic: Boston, MA, 1992; Vol. C, Table 4.2.6.8, pp 219−222.
(52) Creagh, D. C.; Hubbell, J. H. In *International Tables for Crystallography*; Wilson, A. J. C., Ed.; Kluwer Academic: Boston, MA, 1992; Vol. C, Table 4.2.4.3, pp 200−206.
(53) teXsan Crystal Structure Analysis Package; Molecular Structure Corp., The Woodlands, TX, 1992.
(54) Sheldrick, G. M. XPREP, version 5.03; Siemens Industrial Automation, Inc., Madison, WI, 1995.
(55) Sheldrick, G. M. SADABS; Siemens Industrial Automation, Inc., Madison, WI, 1996.